Journal of Materials Chemistry B

Accepted Manuscript

ROYAL SOCIETY OF CHEMISTRY

www.rsc.org/materialsB

Phosphorylated poly(sebacoyl diglyceride) - a phosphate functionalized biodegradable polymer for bone tissue engineering

Peng Huang,[#a] *Xiaoping Bi,*[#b] *Jin Gao,*[c] *Lijie Sun,*[a] *Shaofei Wang,*[a] *Shuo Chen,*[a] *Xianqun Fan,*[**b] *Zhengwei You,*[**a] *Yadong Wang*[*c]

[a] State Key Laboratory for Modification of Chemical Fibers and Polymer Materials, College of Materials Science and Engineering, Donghua University, 2999 North Renmin Road, Shanghai 201620, P. R. China

[b] Department of Ophthalmology, Shanghai Ninth Peoples' Hospital affiliated to Shanghai Jiao Tong University, School of Medicine, 639 Zhizaoju Road, Shanghai, 200011, P.R.China

[c] Departments of Bioengineering, Chemical Engineering, Surgery, and the McGowan Institute, University of Pittsburgh, 3700 O'Hara Street, Pittsburgh, PA 15261, USA

[#] These individuals contributed equally.

[**] Co-corresponding authors. E-mail: Fanxq@sh163.net or zyou@dhu.edu.cn.

[*] Corresponding author. E-mail: yaw20@pitt.edu. Tel: 1-412-624-7196. Fax: 1-412-383-8788.

Abstract

Phosphorylated polymers are promising for bone regeneration because they may recapitulate the essence of phosphorylated bone extracellular matrix (ECM) to build an instructive environment for bone formation. However, most of the existing synthetic phosphorylated polymers are not fully biodegradable; thus, they are not ideal for tissue engineering. Here, we designed and synthesized a new phosphorylated polymer, poly(sebacoyl diglyceride) phosphate (PSeD-P), based on the biodegradable osteoconductive backbone PSeD. To our knowledge, PSeD-P is the first polymer to integrate the osteoinductive moiety β-glycerol phosphate (β-GP). PSeD-P shows good biodegradability and can be readily fabricated on 3D porous scaffolds. It has a porous structure with interconnected macropores (75-150 μm) and extensive micropores (several microns). PSeD-P promotes the adhesion, proliferation, and maturation of osteoblasts more effectively than poly(lactic-*co*-glycolic acid) (PLGA). Furthermore, PSeD-P induces a significantly higher expression of osteogenic biomarkers and ALP activity in mesenchymal stem cells (MSCs) compared to its non-phosphorylated precursor, PSeD. The level of improvement is comparable to free β-GP in culture medium. More importantly, without using β-GP, the typical mineralization promoter in osteogenic culture media, PSeD-P substantially induces mineralized ECM in MSCs, which is totally absent using PSeD under identical culture conditions. PSeD-P provides a new strategy to integrate bioactive phosphates via β-GP into biomaterial, and has promise for bone regeneration applications. In addition, the synthetic method is versatile; both the backbone and the side phosphate groups could be readily tailored to generate a family of phosphorylated polymers for a wide range of biomedical applications.

Keywords: phosphorylated polymer, β-glycerol phosphate, osteogenesis, mineralization, bone regeneration

1. Introduction

Non-union bone defects have no satisfactory clinical solutions. Bone tissue engineering provides a promising approach to address this challenge.[1] Scaffold materials are the key to this approach, especially in emerging cell-free *in situ* bone regeneration.[2] Although significant advances have been made, few materials have led to clinical success. Thus, new materials are needed. Biomimetic materials that can mimic the structure and function of the native bone matrix are expected to be part of the next generation of materials. Among these, phosphorylated materials are an important class because bone is a highly phosphorylated tissue. Many studies show that phosphate is able to induce calcium deposition and plays a key role in extracellular matrix (ECM) mineralization.[3,4] However, most of the existing phosphorylated materials are inorganic. They are usually brittle and hard to process and degrade. Their structures and consequent properties are difficult to control.[5] Synthetic polymers have also been widely used in bone tissue engineering due to their reproducible and controllable structures, wide and tunable physical and mechanical properties, relative ease of processing, and low risk of toxicity, immunogenicity and infection.[6] Most synthetic polymers are biologically inert.[6,7] Phosphorylated polymers may combine the aforementioned advantages of polymeric biomaterials and the potential biomimetic bioactivity derived from phosphate. Phosphorylated polymers are expected to recapitulate the essence of phosphorylated proteins to efficiently promote mineralization and mimic the organic/inorganic hybrid bone matrices to build an environment for bone formation.[7,8] Upon degradation, phosphorylated polymers could release phosphate, which is critical for ECM mineralization and ossification, a crucial step of bone formation.[9,10] Thus, phosphorylated polymers hold great promise for bone regeneration.[7,8] Some polymers with pendent phosphate groups have been shown to promote the osteogenesis of MSCs.[8,11,12] However, existing phosphorylated polymers mainly have carbon-carbon backbones, such as polymethacrylate and polyvinyl alcohol moieties.[11-13] Thus, they are essentially not fully biodegradable, which limits their application in bone tissue engineering.[7] New biodegradable phosphorylated polymers are desired for their use in bone regeneration.

Here, we report a new phosphorylated polymer, poly(sebacoyl diglyceride) phosphate (PSeD-P), for bone regeneration (Fig. 1). This polymer is designed according to the following considerations: (I) Osteocompatible backbone. The backbone is based on an osteocompatible polymer - PSeD, which was recently

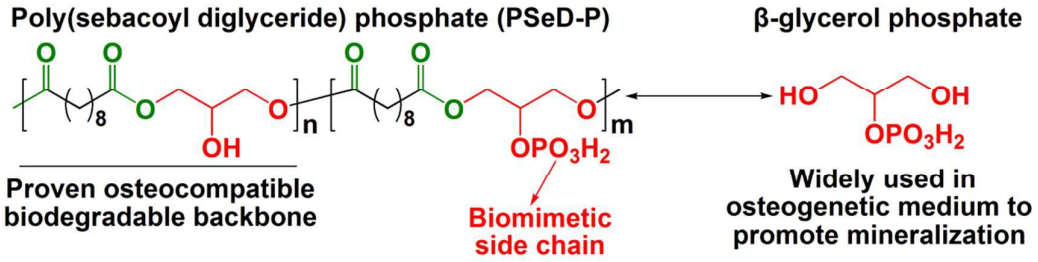

Fig. 1. Design of the phosphorylated polymer PSeD-P for bone regeneration.

developed by our group.[14] PSeD has been shown to promote the mineralization of osteoblasts and the human mesenchymal stem cell extracellular matrix, and it exhibits excellent *in vitro* and *in vivo* biocompatibility and biodegradability.[15] In addition, PSeD is a refined version of another widely used polymeric biomaterial, poly(glycerol sebacate) (PGS). PGS has been shown to support the osteogenic phenotype of osteo-precursor cells *in vitro* and could fully regenerate a rabbit ulna critical size defect *in vivo*.[16,17] (II) Biomimetic pendent phosphate groups. Free dihydrogen phosphate ($-PO_4H_2$) groups are attached to the main chain via a phosphoester bond, which can be readily cleaved via hydrolytic degradation and biodegradation by alkaline phosphatase (ALP). The chemical nature of the phosphorus-containing moiety of materials plays a key role in mineralization.[8] For example, poly(phosphazene), one of the most extensively investigated phosphorus-containing polymers, shows little effect on mineralization, possibly due to the unfavorable nature of backbone phosphorus.[8] Dihydrogen phosphate has been shown to be one of the most efficient inducers of mineralization, among various organic functional groups.[8] In PSeD-P, the pendent phosphate groups mimic the native structure of the phosphorus-containing moiety and retains the corresponding bioactivity. (III) Bioactive degradation products. Different from previously reported phosphorylated polymers, PSeD-P integrates an osteoinductive moiety, β-GP, by biodegradable ester bonds. It is expected to release β-GP upon degradation. β-GP has been widely used in osteogenic media to provide phosphate for the mineralization of osteoblasts and stem cells.[18,19] β-GP serves as the substrate of ALP producing inorganic phosphate by hydrolysis, which could effectively induce calcium deposition in the culture medium.[19]

Thus, we expect that PSeD-P can combine the beneficial effects of PSeD, $-PO_4H_2$ groups, and β-GP to promote osteogenesis, mineralization and eventual bone regeneration. Here, we report the detailed synthesis, fabrication, and characterization

of PSeD-P and its porous scaffold. Furthermore, we systematically investigated the interactions between PSeD-P and MSCs and demonstrated its ability to promote osteogenesis and ECM mineralization.[20]

2. Materials and methods

2.1 The synthesis and characterization of PSeD and PSeD-P

Chemical Reagents: Sebacoyl chloride (TCI, 90%) was distilled under reduced pressure. Sebacic acid (J & K, 99%) was recrystallized three times from ethanol and dried under vacuum. Tetrahydrofuran (THF, Sinopharm Chemical Reagent Co., Ltd., China, HPLC) was dried with a sodium wire and distilled. Anhydrous glycerol (Sigma Aldrich, ≥99.5%), trifluoroethanol (CF_3CO_2H, J & K, >99.8%), and phosphorus oxychloride ($POCl_3$, Sinopharm Chemical Reagent Co., Ltd., China, ≥99.0%) were used as received. Triethylamine (Alfa Aesar, 99%) was dried by anhydrous NaOH and distilled. Anhydrous N,N-dimethylformamide (DMF) was purchased from J & K. Ethyl ether, ethyl acetate, and acetone were purchased from Sinopharm Chemical Reagent Co., Ltd., China. Deuterated solvents for NMR analysis were purchased from Cambridge Isotope Laboratories, Inc. All solvents were used without further purification.

2.1.1 Synthesis of PSeD

PSeD was synthesized via a method that was slightly modified from our previous reports.[14,21] Briefly, an equimolar amount of diglycidyl sebacate and sebacic acid reacted in the presence of 0.6 mol.% tetrabutylammonium bromide in anhydrous N,N-dimethyl formamide (DMF) at 95 ^{o}C for 24 h. The reaction mixture was purified via precipitation in ethyl ether and was vacuum-dried to yield PSeD.

2.1.2 Synthesis of PGS

PGS was synthesized according to a previous report.[22] Recrystallized sebacic acid and anhydrous glycerol were added to a 500-ml three-neck flask. The reactants were steadily heated to 120 ℃ with bubbling N_2 passing through. The mixture was stirred at 120 ℃ for 24 h before the N_2 bubbler was removed and vacuum was applied. The reaction mixture continued to stir at 1 Torr and 120 ℃ for another 24 h. The resultant polymer was a pale yellow, highly viscous semi-solid.

2.1.3 Synthesis of PSeD-P

An anhydrous THF (4 ml) solution of $POCl_3$ (230.8 mg, 1.506 mmol, 0.5 eq based on the theoretical amount of hydroxyl groups in PSeD) was added dropwise to

an anhydrous THF (11 ml) solution of PSeD (802.3 mg, 3.110 mmol) under a nitrogen atmosphere at -15 ^{o}C. After addition, the mixture was warmed to room temperature and stirred for another 12 h. Then, it was quenched with de-ionized water and concentrated on a rotary evaporator. The raw product was redissolved in acetone, precipitated in de-ionized water, and dried under vacuum at room temperature to yield PSeD-P (586.0 mg) as a solid.

2.1.4 Polymer characterization

The molecular weights and their distribution were determined via Waters gel permeation chromatography (GPC) with a differential refractive index detector and a Brookhavend multi-angle light scattering detector. The measurement was performed at 40 ^{o}C using THF (HPLC grade) as the eluent. The ^{1}H NMR, ^{13}C NMR, ^{31}P NMR spectra were recorded on a Bruker 400 NMR. The attenuated total reflectance-Fourier transformed infrared (ATR-FTIR) spectrum was recorded on a Thermo Nicolet 6700 spectrometer. Inductively coupled plasma atomic emission spectra (ICP-AES) were recorded on a Leeman Prodigy ICP spectrometer. The samples were degraded via nitric acid before the ICP test. For the measurement of static air-water contact angles, glass slides were coated with a THF solution of PSeD-P or PSeD. The glass slides were dried at room temperature under 1 Torr for 24 h after the solvent was evaporated in air to produce a thin film of PSeD-P or PSeD. Then, the contact angle of the film was recorded on a contact angle instrument (Contact Angle SystemOCA40, Dataphysics Co., Germany) at room temperature. Five measurements were performed and averaged for each sample.

2.1.5 *In vitro* degradation of PSeD-P

An *in vitro* enzymatic degradation test was performed using the lipase enzyme from *Thermomyces lanuginosus* (100,000 U/g, Sigma) at an activity of 2000 U/ml in Dulbecco's phosphate buffered saline (PBS).[23] PSeD-P was cured at 150 ^{o}C and 1 Torr for 24 h to obtain PSeD-P block material. Disk-shaped samples (4 mm in diameter by 1.2-mm thickness) were weighed and placed in the aforementioned lipase solution (6 ml/sample) and incubated at 37 ^{o}C. The lipase solution was changed after 5 h to maintain the concentration of the lipase enzyme. At the predetermined harvest times, samples were retrieved, washed with deionized water and vacuum dried overnight at 60 ^{o}C. The degree of degradation was determined by the change in dry weight. Three replicates were averaged.

2.2 Fabrication and characterization of the PSeD-P scaffold

2.2.1 Fabrication of the scaffold

Porous scaffolds of PGS/PSeD-P/PSeD were prepared by a modified salt fusion method.[24] The process is briefly described below, using PSeD-P as an example. Salt particles with a size range of 75 to 150 μm were placed into a mold consisting of three components: a Teflon-coated stainless-steel disk, a Teflon-coated ring-shaped steel shim, and permanent magnets to join the assembly. The thickness of the final scaffold was 1 mm and was controlled by the corresponding shim. The molds were transferred to and kept in a humidity chamber at 37 °C and 85% relative humidity for 1.5 h. The fused salt templates were dried in a vacuum oven at 120 °C and 1 Torr for 2 h. The aforementioned (2.1.2) PSeD-P reaction mixture in THF was added to the salt mold. The THF was allowed to evaporate in a fume hood for 30 min. The mold was transferred to a vacuum oven and cured at 150 ^{o}C under 1 Torr for 24 h. The resultant PSeD-P-impregnated salt template was soaked in deionized water for 24 h, with the water changed three times. Then, the scaffold was lyophilized.

2.2.2 Morphology of the PSeD-P scaffold

The porosity of each scaffold was determined according to the following equation: Porosity (%) = $(\rho_{PSeD\text{-}P} - \rho_d) / \rho_{PSeD\text{-}P} \times 100$. The apparent density ($\rho_d$) of each scaffold was calculated from its dry weight and volume. The scaffolds were typically 1.0 mm thick and 10.5 mm in diameter. The true density ($\rho_{PSeD\text{-}P}$) of the PSeD-P scaffold was 1.2848 g/cm^3, which was measured by the density analyzer (UL TRAPYCNOMETER 1000, Quantachrome) at 25 °C. The results of 10 scaffolds were averaged.

The scaffold was mounted on aluminum stubs that were sputtered with gold. Then, the morphology of the scaffolds was investigated by environmental scanning electron microscopy (ESEM, Quanta-250, FEI, USA).

2.2.3 Thermal properties of the PSeD-P scaffold

Thermogravimetry analysis of the PSeD-P scaffold was performed on a Discovery TGA (TA, American) from 40 ^{o}C to 500 ^{o}C at a heating rate of 10 ^{o}C/min under a nitrogen atmosphere. Differential scanning calorimetry (DSC) was performed on a NETZSCH DSC 204 F1 Phoenix from -50 ^{o}C to 150 ^{o}C at a heating rate of 10 ^{o}C/min under a nitrogen atmosphere. The glass transition temperature (T_g) was defined as the midpoint of the glass transition and was determined by the analysis software from NETZSCH.

2.2.4 Mechanical properties of the PSeD-P scaffold

The mechanical properties of the PGS/PSeD/PSeD-P scaffolds were evaluated by compression tests using an Instron 5969 universal testing machine with a 5 N sensor. Disk-shaped specimens (10.5 mm in diameter by 1-mm thickness) were punched from the PSeD-P scaffold. Each specimen was compressed to a strain of 40% at a rate of 1.00 mm/min with an initial load of 0.01 N. The compression modulus was calculated by taking the initial slope of the stress-strain curve. The data from 5 specimens were averaged. In the cyclic compression test, the sample was compressed to a strain of 40% and then allowed to recover to 5% before immediately compressing to a strain of 40% at a rate of 1.00 mm/min 10 times.

2.3 Material - osteoblast interaction

2.3.1 Preparation of the polymer surface for cell culture

To prepare the polymer surface for cell culture, tissue culture treated polystyrene (TCPS) surfaces were coated with PSeD-P as follows. A 2,2,2-trifluoroethanol solution of polymer (1 g/l) was filtered through a 0.2-μm filter and added to 24-well (80 μl/well) or 96-well (20 μl/well) TCPS plates. The plates were dried under vacuum overnight after evaporation of the solvent in air, sterilized by UV light for 30 min, and washed with phosphate buffered saline (3 × 1 ml/well for 24-well plate, 3 × 100 μl/well for 96-well plate) and culture medium (1 × 1 ml/well for 24-well plate and 1 × 100 μl/well for 96-well plate) with gentle shaking before use. PSeD and PLGA (5050DLG 5E, Lakeshore Biomaterials, Birmingham, AL, USA) coating on TCPS surfaces were used as controls and prepared in the same manner as the PSeD-P coating.

2.3.2 Cell culture

Osteoblasts were isolated by sequential trypsin-collagenase digestion of calvaria obtained from neonatal (2-3 days old) Sprague-Dawley rats.[25] All animal-related experiments were performed in compliance with a protocol approved by the Institutional Animal Care and Use Committee (IACUC) at the University of Pittsburgh. Cells were cultured in a fully humidified incubator (37 ^{o}C, 5% CO_2). The culture medium was changed 1 day after isolation and every subsequent third day. Within approximately 5-7 days, cells reached subconfluency and were passaged. Passage 4 osteoblasts were used for all of the cell function tests.

2.3.3 Cell morphology

Osteoblast single cell suspensions (2×10^4 cells/well) were cultured on PSeD-P,

PSeD and PLGA surfaces in 24-well plates in a humidified incubator. F-actin fluorescence images were captured to show the cytoskeleton structure 24 h after cell seeding. Briefly, after fixing cells for 10 min with 4% paraformaldehyde and after subsequent 5 min permeabilization with 0.1% triton-X 100, 2% bovine serum albumin (BSA) was used to block nonspecific protein interactions for 30 min at room temperature. Then, cells were incubated in rhodamine phalloidin (Cytoskeleton, #PHDR1, 14 μM stock solution was 1:200 diluted in 0.5% BSA) for 30 min at room temperature (in darkness). Nuclei were stained with DAPI for 20 min at room temperature (in darkness). Cells were rinsed with PBS (3 × 1 ml) between each step. Fluorescent micrographs at a 594-nm emission were taken using the Nikon Eclipse Ti microscope.

2.3.4 Cell adhesion

The cell adhesion rate was used as a quantitative evaluation of osteoblast adhesion onto PSeD-P, PSeD and PLGA coated 24-well TCPS plates (n = 5). Osteoblasts were cultured for 2, 4 and 24 h on the polymer-coated plates, and at each time point, the adhered osteoblasts were enzymatically (0.25% trypsin-0.1% EDTA; Gibco) detached and counted using a hemocytometer. The cell adhesion rate was expressed as a percentage of the initial number of seeded cells (2×10^4 cells/well).

2.3.5 Cell proliferation

The proliferation of osteoblasts on PSeD-P, PSeD and PLGA was estimated using the (3-(4,5)-dimethylthiazol-2,5-diphenyltetrazolium bromide) (MTT) assay. Osteoblasts were seeded on PSeD-P, PSeD and PLGA surfaces in 96-well plates (2000 cells/well, n = 8 per surface per time point). The medium was removed and replaced with 100 ml of MTT solution (freshly prepared with 5 mg of MTT powder in 1 ml of DMEM without phenol red) at predetermined time points. Following incubation for 4 h in a fully humidified incubator, the water-soluble MTT was taken up by active cells and converted to insoluble purple formazan granules in mitochondria. Subsequently, 100 μl of a sodium dodecyl sulfate solution (1 g dissolved in 10 ml of 0.01 M HCl) was added to dissolve the precipitated formazan at 37 ^{o}C for 18 h. The absorbance at a wavelength of 570 nm was measured by a SynergyMX plate reader (Biotek, Winooski, VT). The analytical assays were performed every two days until 7 days after cell seeding.

2.3.6 Alkaline phosphatase activity assay

ALP activity was measured using a commercial kit (Sigma, #P7998). The kit

uses p-nitrophenylphosphate (pNPP) as a phosphatase substrate, which turns yellow when dephosphorylated by ALP. Osteoblasts were seeded on PSeD-P, PSeD and PLGA in 24-well plates (2×10^4 cells/well, n = 5) and continuously cultured for 7, 14 and 21 days for ALP activity assays. Briefly, at each time point, 200 µl of cell lysis solution (performed with a Sigma kit, #C2978) with 2 µl of Protease Inhibitor Cocktail (Thermo Scientific, #87786) was added to each well after removing the culture medium and rinsing with PBS 3 times. After a 15-min equilibration on ice, the cells were scraped, and the lysis solution was collected in eppendorf tubes and centrifuged (13,362 × g) at 4 ^{o}C for 15 min. Ten microliters of the supernatant was mixed with 100 µl of pNPP reagent and reacted at room temperature in darkness for 30 min to produce a soluble end product, which was yellow and was spectrophotometrically quantified at 405 nm using a SynergyMX plate reader (Biotek, Winooski, VT). The ALP activity was normalized according to total protein concentration (Pierce 660 nm protein assay Kit, Thermo Scientific) and time.

2.4 Polymer-hMSCs interaction

2.4.1 hMSCs culture

hMSCs (passage 1 from the vertebrae of cadaveric bodies) were kindly provided by Prof. Albert D. Donnenberg at the University of Pittsburgh School of Medicine.[26] hMSCs were cultured on PSeD-P, PSeD and PLGA surfaces with α-modified minimal essential medium (α-MEM, Cellgro) supplemented with 15% fetal bovine serum (FBS, Lonza), 10,000 U/ml penicillin and 10,000 U/ml streptomycin (Sigma, USA), and they were incubated at 37 °C in a high humidity environment containing 5% CO_2. The medium was replaced every 2 days, and the cells were passaged at approximately 80% confluence. hMSCs in the second passage were prepared for the following experiments.

2.4.2 hMSCs differentiation test

The osteogenic differentiation of hMSCs was assessed by the detection of osteogenic biomarker collagen type I (Col I). hMSCs were seeded onto PSeD-P and PSeD coated 24-well TCPS at a density of 2×10^4/well with proliferation medium (α-MEM with 15% FBS) for the first 24 h. Then, the culture medium was changed to differentiation medium (α-MEM supplemented 15% FBS, 10^{-5} mM dexamethasone, and 0.2 mM ascorbic acid. β-GP (5 mM) was added to the medium on some of the PSeD surfaces as the positive control. All culture medium was changed every 2 days. After 7 days of culture, a portion of the hMSCs were fixed in phosphate-buffered 2%

paraformaldehyde for immunofluoresence staining. The remaining cells were continuously cultured for 21 days, and the multilayer cells were re-plated separately on a glass-bottom 3.5-cm petri dish at a density of 2×10^4/ml for 24 hours for further immunofluoresence staining.

Immunofluoresence staining for Col I was used to detect the osteogenic differentiation of hMSCs. Briefly, cells were fixed in phosphate-buffered 2% paraformaldehyde for 15 min at room temperature and permeabilized with 0.1% triton-X 100. Non-specific epitopes were blocked by incubation in 2% BSA for 1 h at room temperature, followed by incubation with primary antibodies against human Col I (Millipore, USA) (1:100 dilution in DPBB (0.5% BSA in PBS)) at 4 ^{o}C overnight in a wet chamber. Bound primary antibodies were detected with FITC-conjugated goat anti-rabbit IgG for Col I (Santa Cruz Biotechnology) as a secondary antibody for 60 min at room temperature. DAPI was used to stain nuclei for 20 min. Cells were rinsed with PBS 3 times and with DPBB 2 times between each step. Fluorescence micrographs were taken using the Nikon Eclipse Ti microscope.

2.4.3 Alkaline phosphatase activity assay

The ALP activity of hMSCs was assayed using a commercial kit (Sigma, #P7998). hMSCs were seeded on PSeD-P and PSeD coated TCPS. After 7 and 14 days culture, hMSCs were lysed and ALP activity was assessed. The detailed methods were as described above (section 2.3.6).

2.4.4 Mineralization of ECM

Alizarin Red S (ARS) Staining was used to detect calcium deposition and mineralization of the ECM after 21 days hMSC culture. The cells were washed twice with PBS and fixed with phosphate-buffered 2% paraformalin for 20 min. Fixed cells were washed 3 times with distilled water and were subsequently stained with 1% ARS in distilled water (PH 4.1~4.3) for 5 min. The remaining dye was removed and washed out with distilled water 3 times. Finally the cells were air-dried for 30 min, and images were captured using a Nikon Eclipse Ti microscope.

2.5 Polymer-rat MSCs interaction on 3D scaffolds

2.5.1 Cell culture on polymer 3D scaffolds

The disc-shaped scaffolds (diameter: 5 mm, thickness: 1 mm) were punched from porous polymer sheets. After autoclaving, the scaffolds were progressively soaked in 70, 50, and 25% ethanol as well as PBS for 30 min each with gentle shaking on an orbital shaker. Then, the scaffolds were washed with PBS again and preconditioned

overnight in cell-culture medium. The scaffolds were transferred to 24-well plates, and the residual culture medium was removed by vacuum. Rat MSCs (rMSCs) were isolated from the femora and tibiae of 8 week old Sprague-Dawley female rat followed the reported protocol.[27] Then, a total of 2×10^5 freshly trypsinized passage 2 rMSCs were seeded on each scaffold in two steps. First, each scaffold received 1×10^5 cells that were suspended in 10 μl of medium on the top and was incubated at 37 ^oC for 30 min. Second, the scaffold was flipped over, and another 1×10^5 cells were seeded as described above. The cell-seeded scaffolds were incubated at 37 ^oC for another 2 h before 1 ml of culture medium (α - MEM supplemented 15% FBS, 10^{-5} mM dexamethasone, and 0.2 mM ascorbic acid) was added to each well. The constructs were cultured in a humidified incubator (37 ^oC, 5% CO_2). The culture medium was changed every two days.

2.5.2 Scanning electron microscopy

The morphology of the constructs was investigated by SEM. At a predetermined time, the constructs were washed with PBS and fixed with 2.5% glutaraldehyde in PBS at ambient temperature for 1 h. After rinsing with PBS for 3 times (15 min/time), the samples were post-fixed with osmium tetroxide for 1 h and immediately rinsed with PBS 3 times. After further rinsing with PBS 3 times (15 min/time), the constructs were dehydrated in a series of PBS-ethanol baths (30, 50, 70, 90% ethanol) for 15 min each and in 100% ethanol three times for 15 min each. Then, the samples were washed with heximethyldisilizane (HMDS) for 15 min and air-dried in a fume hood at room temperature. The samples were mounted on aluminum stubs, sputtered with gold, and viewed with a JEOL JSM6330F SEM. For further elemental composition analysis, the samples were sputtered with gold-palladium and viewed with Philips XL-30 field emission SEM equipped with detectors for SE and BSE imaging and energy-dispersive X-ray spectroscopy (EDS).

2.5.3 Histological analysis

At a predetermined time, the constructs were washed with PBS, fixed in 10% neutral buffered formalin, and embedded in Tissue-Tek optimal cutting temperature compound (Sakura Finetek). Embedded samples were sectioned at an 8-μm thickness. For runt-related transcription factor 2 (Runx2) immunofluoresence staining, primary antibodies against rat Runx2 (1:100; Santa Cruz Biotech, USA) were used, followed by CY3-fab2-conjugated donkey anti-goat IgG (Santa Cruz Biotech, USA) as a

secondary antibody. Nuclei were counterstained with DAPI. Fluorescence micrographs were taken using the Nikon Eclipse Ti microscope.

2.6 Statistical analysis

Statistical analysis was performed using one-way ANOVA and a LSD Post Hoc multiple comparison with a minimum confidence level of $p < 0.05$ for statistical significance. All values are reported as the mean ± standard deviation.

3. Results

3.1 Synthesis and characterization of PSeD-P

PSeD with a number average molecular weight (M_n) of 13.9 kD and a polydispersity index (PDI) of 1.41 was synthesized via acid-induced epoxide ring-opening polymerization between diglycidyl sebacate and sebacic acid according to our previous reports (Scheme 1).[14,21] Partial phosphorylation of the hydroxyl groups of PSeD using phosphorus oxychloride readily produced PSeD-P (Scheme 1). After purification, the collected refined PSeD-P had a M_n of 15.0 kD and a relatively low PDI of 1.16. NMR and FTIR were used to characterize the structure of PSeD-P. In the ^{1}H NMR spectrum (Fig. 2A), the signals marked 'a_1', a_2', and 'a_3' at chemical shift δ 1.32, 1.61, and 2.35 ppm corresponded to the CH_2 protons of the sebacoyl moiety in the polymer backbone. The broad peak marked "-O*H*" at around δ 3.06 ppm indicated the presence of hydroxyl groups. A series of signals marked "b (R=H), c" at δ 3.62-4.36 ppm were ascribed to the protons of the glyceryl moiety. When the free hydroxyl groups was phosphorylated or esterified, the signals of methine protons in glycerol moiety were shifted downfield to δ 5.10-5.27 ppm marked "b (R=-PO_3H_2 or Polymer chain)" due to the electron-withdrawing effect of phosphate or ester groups.[14] The relative integration of different protons was consistent with its structure. The ^{13}C NMR spectrum of PSeD-P corroborated well with the ^{1}H NMR spectrum. The signals of the CH_2 carbons in the sebacoyl moiety appeared at δ 24.58, 28.69, and 33.54 ppm (Fig. 2B). The signals of the carbons in the glyceryl moiety appeared at δ 60.08-75.09 ppm. The signals of the carbonyl carbons in the sebacoyl moiety appeared at δ 174.77 ppm. The strong signal marked 'a' at δ 1.88 ppm in the ^{31}P NMR spectrum confirmed the presence of the phosphate group (Fig. 2C). Comparison of the FTIR spectra of PSeD and PSeD-P clearly revealed the characteristic signal of phosphate groups (the stretch vibration of P=O bonds at 1291 cm^{-1}) (Fig. 2D). In addition, ICP revealed that

the amount of phosphorus in PSeD-P was 1.26% (m/m). This indicated that approximately 10.9% of the free hydroxyl groups in PSeD were converted into phosphate groups.

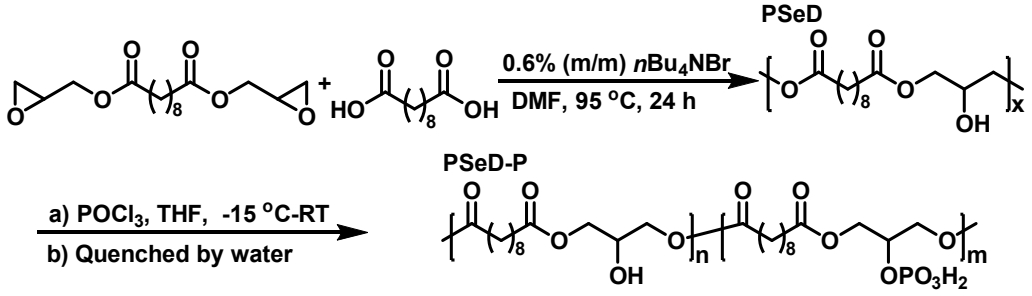

Scheme 1: Synthetic route of PSeD-P

The hydrophilicity of PSeD-P was investigated by measuring the water contact angle of the polymer films. As expected, the introduction of a phosphate group into PSeD significantly increased the hydrophilicity. The static air-water contact angle of the PSeD-P film was only 20.6° ± 4.2°, much lower than the one of PSeD film (49.5 ° ± 2.7°) under an identical condition.

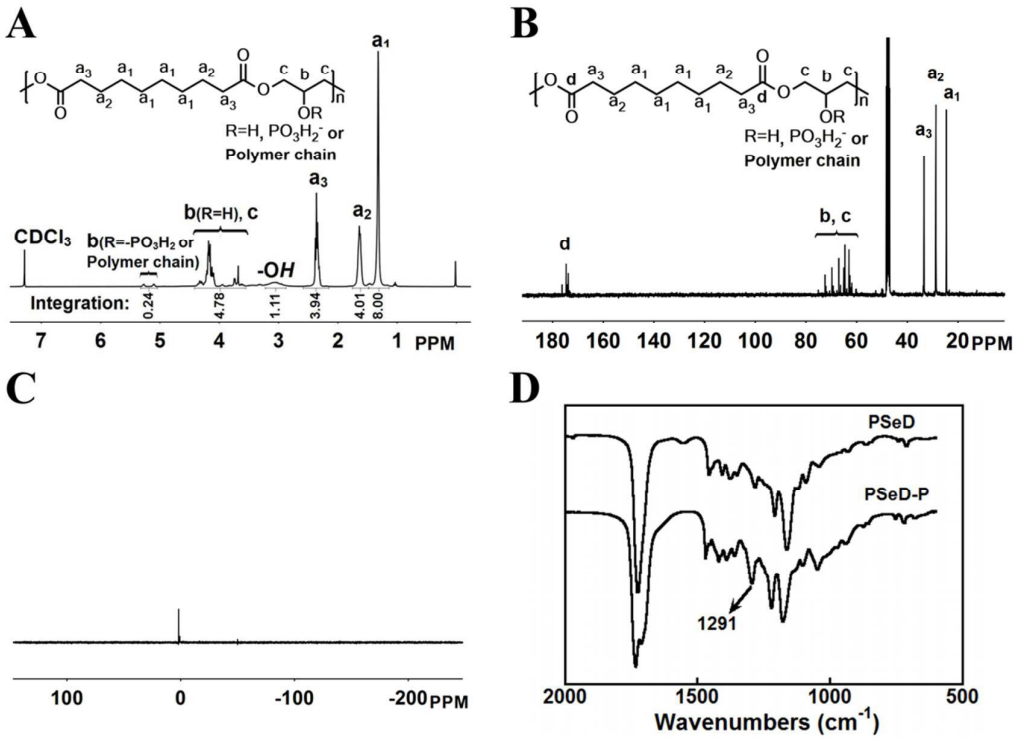

Fig. 2. Structural characterization of PSeD-P. (A) The ^{1}H NMR spectrum (400 MHz, chloroform-*d*) of PSeD-P indicated the presence of the glyceryl moiety at δ 3.62-4.36 ppm (with free hydroxyl groups) and its methine protons at δ 5.10-5.27 ppm (when hydroxyl groups were phosphorylated or esterified), and the structure of the sebacoyl

moiety at δ 1.32, 1.61, and 2.35 ppm. (B) The ^{13}C NMR (100 MHz, methanol-d_4) spectrum of PSeD-P corroborated well with the ^{1}H NMR. The resonance of the glyceryl, sebacoyl, and ester moieties occurred at δ 60.08-75.09 ppm, δ 24.58, 28.69, 33.54 ppm, and δ 174.77 ppm, respectively. (C) The ^{31}P NMR (162 MHz, acetone-d_6) detected a strong signal at δ 1.88 ppm, which confirmed the presence of the phosphate group. (D) The FTIR spectrum PSeD-P displayed the prominent absorption of phosphate P=O bonds at 1291 cm^{-1}.

The backbone of PSeD-P is based on ester bonds. It can be degraded by hydrolysis. Enzymatic digestion can also degrade the PGS backbone both *in vitro* and *in vivo*.[23] We expected that PSeD-P could be degraded in a similar way. For a quick screening of the biodegradability of PSeD-P, we investigated the *in vitro* degradation of cured PSeD-P in a PBS solution of lipases enzymes (2000 units/ml). A continuously significant mass loss was observed. The total 25.3 ± 1.9 % mass was lost within 11 h (Fig. 3). This confirmed the good biodegradability of PSeD-P and indicated the ester groups are likely the primary degradation sites.

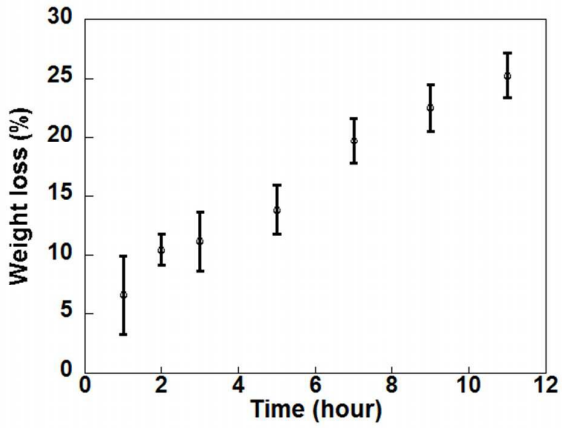

Fig. 3. *In vitro* enzymatic lipase digestion of the cured PSeD-P. PSeD-P degraded gradually in the presence of the lipase enzyme from Thermomyces lanuginosus at an activity of 2000 U/ml in PBS. A mass loss of 25.3 ± 1.9 % was approached within 11 h.

3.2 Fabrication and characterization of the PSeD-P scaffold

We used thermal curing and salt leaching to fabricate a porous PSeD-P 3D scaffold as described previously.[24] As shown in 3.1, only 10.9% of the hydroxyl groups in PSeD were converted into phosphate groups in the purified PSeD-P. This

was relatively low. We speculate that phosphorus oxychloride is too sensitive to moisture, its efficiency is compromised. Furthermore, some PSeD-Ps with high phosphate contents may partly dissolve in water and be washed out during post-treatment. Theoretically, the reactivity of partly hydrolyzed phosphorus oxychloride ($POCl_2OH$ or $POCl(OH)_2$) would be enhanced and could react with the hydroxyl groups of PSeD-P during curing. Furthermore, thermal curing would convert the water-soluble PSeD-P into water-insoluble crosslinked scaffolds as well. Thus, we reasoned that directly using an untreated PSeD-P reaction mixture instead of purified PSeD-P to fabricate the scaffold would enhance the phosphate content in the resultant scaffold. Accordingly, the PSeD-P reaction solution was directly added to salt template and dried. The impregnated template was cured at 150 ^{o}C and 1 Torr for 24 h followed by salt leaching and freeze-drying. As expected, the phosphorus content of the resultant PSeD-P scaffold was significantly higher than in the purified PSeD-P. ICP showed that the PSeD-P scaffold contained 2.55% phosphorus (measured by ICP) indicating that 22.8% of the hydroxyl groups in PSeD were converted into phosphate groups in the resultant PSeD-P scaffold, more than twice the amount observed in purified PSeD-P.

The PSeD-P scaffold had an average porosity of 90.9 ± 0.8%. The morphology of the scaffold was evaluated by SEM (Fig. 4A-C). Macropores (75-150 μm) controlled by porogen (salt particles) were well distributed throughout the scaffold and connected to each other. Interestingly, extensive micropores (several microns) appeared in the macropore walls. It was likely induced by the escape of small molecules, such as glycerol, during curing at high temperature and vacuum.[24] These micropores complement the macropores, and they will likely improve mass transfer and cell communication. Both are critical aspects for engineering 3-D tissues. The thermogravimetry analysis of the PSeD-P scaffold revealed that it was stable up to 300 ^{o}C (Fig. 4D). The DSC curve of the PSeD-P scaffold showed a T_g of -30.6 ^{o}C and no crystallization between -50 ^{o}C and 150 ^{o}C (Fig. 4E). This indicated that the PSeD-P scaffold was amorphous at ambient and body temperatures.

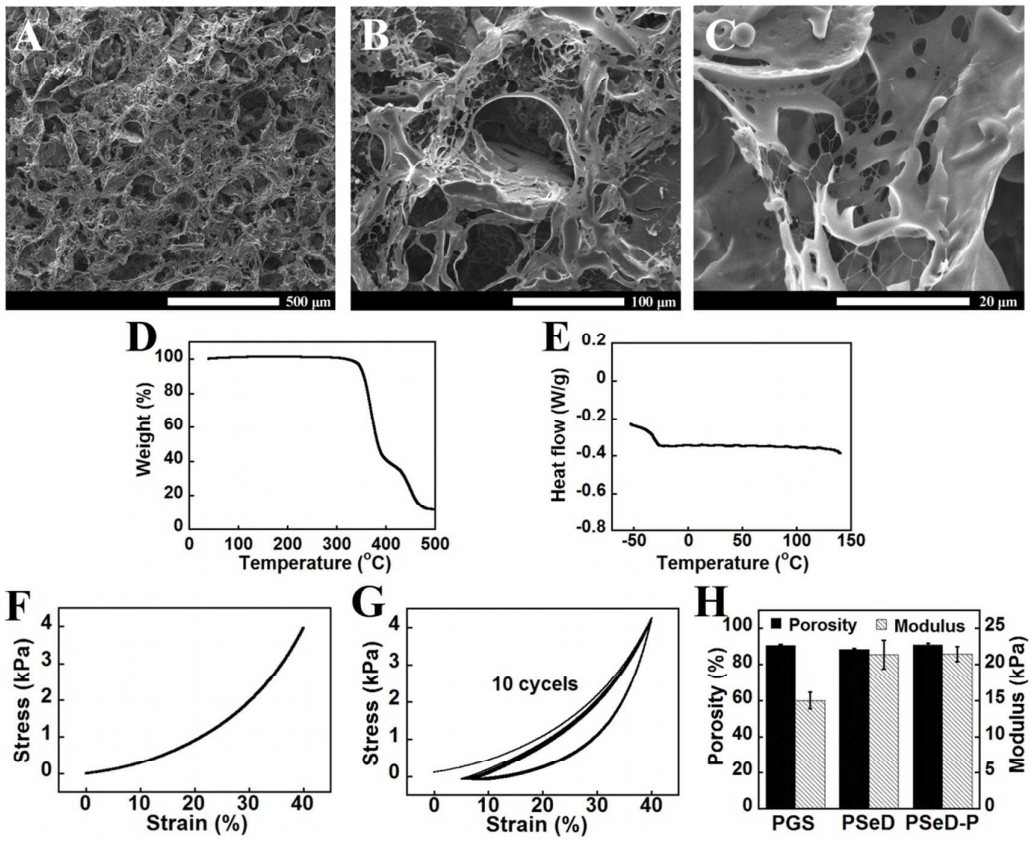

Fig. 4. Characterization of the PSeD-P scaffold. SEM images of the PSeD-P scaffold at different magnifications: (A) 100×, scale bar = 500 μm; (B) 500×, scale bar = 100 μm; and (C) 3000×, scale bar = 20 μm revealed that its hierarchical porous structure with interconnected macropores (75-150 μm) derived from porogen (salt particles) and contained extensive micropores (several microns) throughout the walls of the macropores. This structure is beneficial for cell penetration, cell-cell interactions and mass transport. (D) Thermogravimetry analysis of the PSeD-P scaffold. No thermal decomposition was observed from 40 ^{o}C to 300 ^{o}C. (E) DSC curve of the PSeD-P scaffold. (F) Typical stress vs. strain curve of the PSeD-P scaffold in a simple compression test with a strain up to 40%. (G) Typical stress vs. strain curve of the PSeD-P scaffold in a cyclic compression test with a strain from 5% to 40% for 10 cycles. (H) Comparison of the porosities and compression moduli of PGS/PSeD/PSeD-P scaffolds.

The mechanical properties of the PSeD-P scaffold were investigated by compression testing. The simple compression test revealed that the modulus of the PSeD-P scaffold was 21.47 ± 1.01 kPa (Fig. 4F). Furthermore, cyclic compression

testing with a strain of up to 40% for 10 cycles showed that the PSeD-P scaffold could recover well from dynamic deformation. Only limited hysteresis was observed (Fig. 4G). This revealed that the PSeD-P scaffold was an elastomer at ambient temperature. To further evaluate the mechanical properties of the PSeD-P scaffold, we fabricated PSeD and PGS scaffolds using the same method. The porosities of the PSeD and PGS scaffolds were 88.4 ± 0.6% and 90.6 ± 0.7%, respectively, similar to the porosity of the PSeD-P scaffold (90.9 ± 0.8%) (Fig. 4H). The compression modulus of the PSeD scaffold was 21.36 ± 1.97 kPa, similar to the PSeD-P scaffold (21.47 ± 1.01 kPa) and higher than that of the PGS scaffold (15.00 ± 1.17 kPa).

3.3 PSeD-P - osteoblast interaction

3.3.1 Osteoblast morphology

F-actin staining was used to investigate the morphology of cells cultured on PSeD-P (Fig. 5A-C). Osteoblasts adhered, expanded well, and displayed typical polygonal and poditic shapes on all of the polymer surfaces. Clear microfilaments (F-actin) of osteoblasts were observed, which indicated that PSeD-P was a good substrate for osteoblasts comparable to its precursor, PSeD, and standard biocompatible polymer PLGA.

3.3.2 Osteoblast adhesion

Adhesion of osteoblasts on PSeD-P was evaluated by monitoring the number of cells adhered onto the polymer surfaces at different time points after seeding (Fig. 5D). The number of adhered cells significantly increased within 24 h on all of the polymer surfaces, and the adhesion rate of osteoblasts on PSeD-P reached 77.0 ± 3.8%, higher than that on PLGA (64.0 ± 7.3%).

3.3.3 Osteoblast proliferation

The osteoblast proliferation on PSeD-P was evaluated by the MTT assay (Fig. 5E). The number of metabolically active osteoblasts on PSeD-P significantly increased with the time of culture and was significantly higher than it was on the control polymer PLGA at day 3, 5, and 7 post-seeding. This indicates that PSeD-P had good cytocompatibility with osteoblasts, similar to PSeD, and a stronger ability to promote osteoblast proliferation than PLGA.

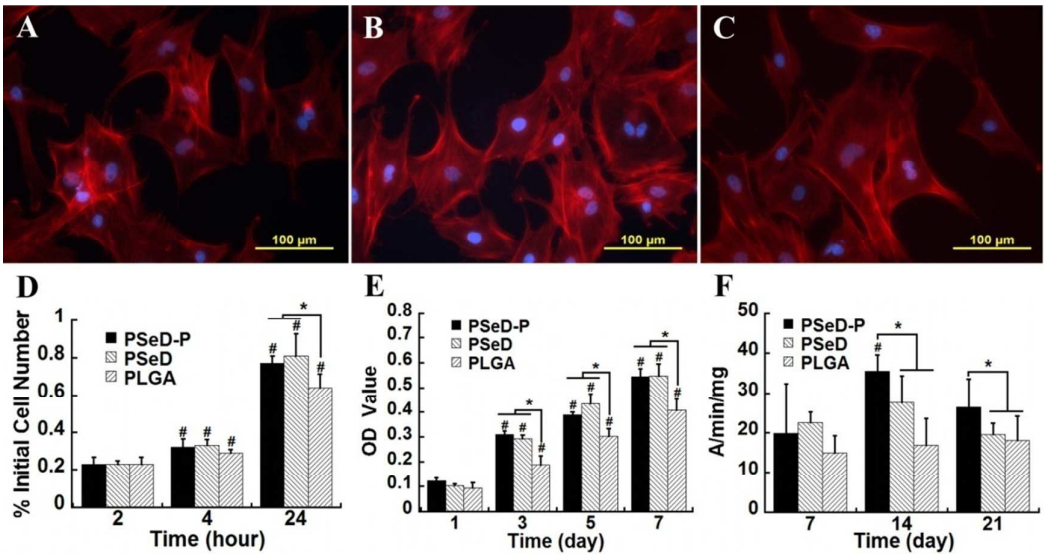

Fig. 5. (A-C) Fluorescence images of F-actin stained osteoblasts 24 h after seeding onto PSeD-P (A), PSeD (B), and PLGA (C). Osteoblasts attached, spread well, and exhibited a typical polygonal morphology on all of the surfaces (magnification 100×, scale bar = 100 μm). (D) Osteoblast adhesion rates on PSeD-P, PSeD, and PLGA surfaces. More osteoblasts adhered on PSeD-P and PSeD than on PLGA 24 h after seeding under an identical condition. (E) MTT assay of osteoblasts cultured on PSeD-P, PSeD, and PLGA surfaces. The optical density (OD value) was proportionate to the number of metabolically active osteoblasts. The OD values on PSeD-P and PSeD significantly increased after another day within 7 days and were both significantly higher than those on PLGA. The results indicate that PSeD-P and PSeD promoted better osteoblast proliferation than PLGA. (F) The ALP activity of osteoblasts on PSeD-P significantly increased from day 7 to day 14 post-seeding and was significantly higher than on PSeD and PLGA at day 14 and day 21 in culture. These results revealed that PSeD-P promoted better maturation of osteoblasts. ALP activity was normalized based on the total protein concentration and time. *: Statistically significant difference between different materials at the same time point ($P < 0.05$); #: statistically significant difference between different time points on the same polymer surface ($P < 0.05$).

3.3.4 Alkaline phosphatase activity

The ALP activity assay was used to evaluate the maturity and function of osteoblasts on PSeD-P (Fig. 5F). The ALP activity of osteoblasts on PSeD-P notably increased from day 7 to day 14 and was significantly higher than on PSeD and PLGA

at day 14 and day 21. This shows that PSeD-P was a good substrate to promote the maturity of osteoblasts.

3.4 PSeD-P & hMSCs 2D interaction

The ability of PSeD-P to promote osteogenesis was evaluated by the interaction of PSeD-P and human mesenchymal stems cells (hMSCs) (Fig. 6). hMSCs are among the most widely used stem cell types in bone tissue engineering.[28,29] Because PSeD-P was designed to mimic the function of β-GP, hMSCs were cultured on the PSeD-P surface without using free β-GP in culture medium. The non-phosphorylated precursor PSeD was used under the same conditions as a negative control. PSeD with 5 mM β-GP in culture medium was used as positive control.

3.4.1 Osteogenic differentiation of hMSCs

Osteogenic differentiation of hMSCs on different polymer surfaces was assessed by the immunohistochemical staining of the osteogenic biomarker Col I. Col I, one of the major components of bone matrix,[9] was highly expressed in the positive control (Fig. 6A, PSeD surface with 5 mM β-GP) and on the PSeD-P surface (Fig. 6B), but it was less expressed on the PSeD surface without β-GP in the medium (Fig. 6C) 7 days after seeding. The maturity and function of differentiated hMSCs were further evaluated based on the ALP activity, a widely used biomarker of osteogenesis and bone formation (Fig. 6D).[30] There were no significant differences between the ALP activities of hMSCs on PSeD-P and PSeD without β-GP in culture medium at an early time point (7 days). However, the ALP activity of hMSCs on PSeD-P significantly increased from day 7 to day 14. After a 14-day culture, hMSCs seeded on PSeD-P (without β-GP) showed much higher ALP activity than those on PSeD using the same culture medium, and the activity was comparable to that of PSeD with 5 mM β-GP in the culture medium. These results show that PSeD-P can resemble the function of free β-GP and promote osteogenic differentiation and maturation.

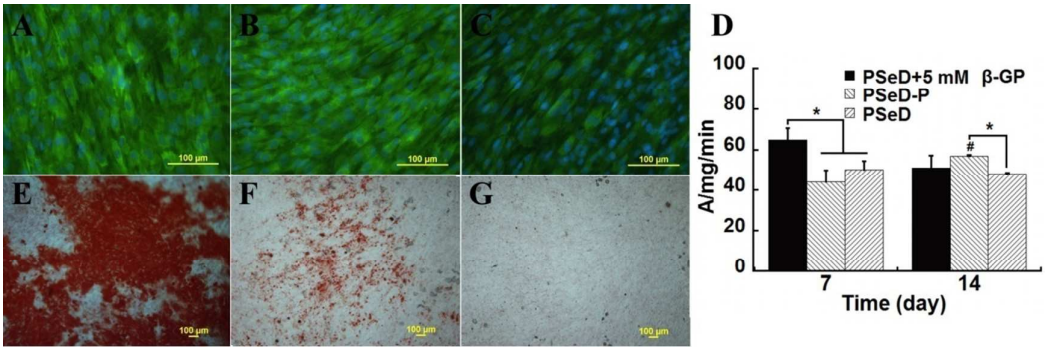

Fig. 6. PSeD-P substantially induced osteogenic differentiation of *hMSCs* and the

mineralization of their ECM. (A-C) Immunofluorescence images of Col I (green) of hMSCs cultured under different conditions for 7 days. Nuclei were counterstained with DAPI (blue) (magnification 100×, scale bar = 100 μm). hMSCs cultured both on positive control (A, PSeD with 5 mM β-GP in culture medium) and PSeD-P (B) expressed Col I, while less Col I positive hMSCs were detected on PSeD (C) without β-GP treatment. (D) ALP activity of hMSCs cultured under different conditions. The ALP activity of hMSCs on PSeD with 5 mM β-GP in culture medium was higher than on PSeD and PSeD-P without β-GP in the culture medium after 7 days. After 14 days, the ALP activity of hMSCs on PSeD-P without β-GP significantly increased, surpassing the results for PSeD with 5 mM β-GP in the culture medium, and was higher than PSeD without β-GP. *: Statistically significant difference between different conditions at the same time point ($P < 0.05$); #: statistically significant difference between different time points under same condition ($P < 0.05$). (E-G) ARS staining of hMSCs at day 21 post-seeding. ECM mineralization (red) of hMSCs was observed on the positive control (E, PSeD with 5 mM β-GP) and PSeD-P surface without β-GP (F). Under identical conditions, no positive red-stained area was found on the PSeD surface without β-GP (G).

3.4.2 Mineralization of ECM

The mineralization of ECM was measured by ARS staining after 21 days of hMSC culture under different conditions (Fig. 6E-G). Even without β-GP treatment, apparent mineralized ECM formed on the PSeD-P surface (Fig. 6F), but was totally absent on the PSeD surface (Fig. 6G). As expected, adding free β-GP to the culture medium led to significant ARS positive areas that were stained red (Fig. 6E). These results show that PSeD-P has an intrinsic ability to promote ECM mineralization, resembling the external mineralization promoter β-GP.

3.5 Preliminary study of the PSeD-P & rMSCs 3D interaction

rMSCs were seeded onto the PSeD-P porous scaffold to evaluate the efficiency of PSeD-P for 3D culture and eventually for *in vivo* applications. rMSCs attached and spread well on the PSeD-P porous scaffolds (Fig. 7). Cells significantly proliferated and infiltrated into the scaffold within 14 days (Fig. 7A-C). Cells in the PSeD-P scaffolds expressed significantly higher levels of Runx2, an essential transcription factor that is associated with osteoblast differentiation compared to cells on a PSeD scaffold at day 14 (Fig. 7D-E). These results show that the PSeD-P scaffold provides

an instructive environment for MSC and could promote osteogenesis better than its non-phosphorylated precursor PSeD.

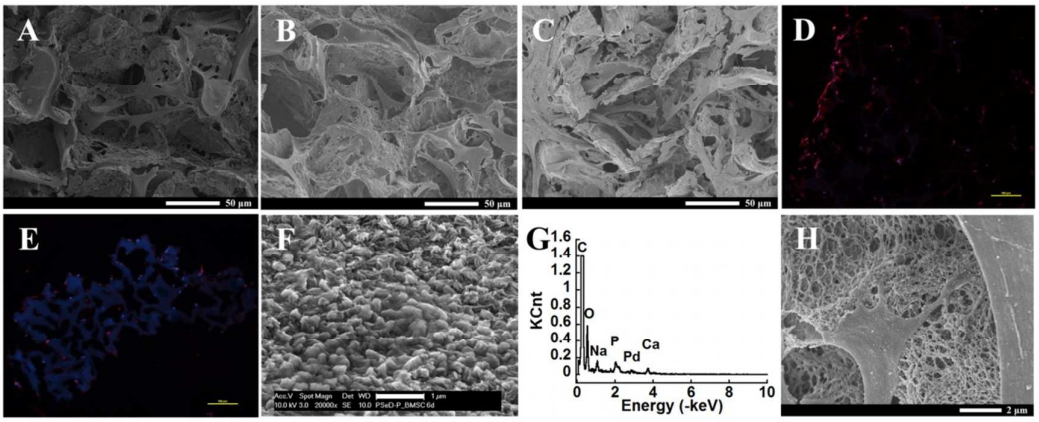

Fig. 7. 3D culture of rMSCs on PSeD-P porous scaffolds. (A-C) SEM images of rMSCs on PSeD-P scaffolds at day 1 (A), day 7 (B), and day 14 (C) after seeding. (magnification 500×, scale bar = 50 μm). (D-E) Fluorescence images of Runx2 staining (red). Runx2 is a typical osteogenic biomarker for rMSCs cultured on PSeD-P (D) and PSeD (E) at 14 days. Nuclei were counterstained with DAPI (blue) (magnification 100×, scale bar = 100 μm). (F) Representative SEM image of the PSeD-P scaffold cultured with rMSCs at day 6 reveals extensive nanocrystals on the surface of the PSeD-P scaffold (magnification 20,000×, scale bar = 1 μm). (G) EDX analysis shows that these nanocrystals contain calcium and phosphorus, indicating ECM mineralization in the rMSCs. (H) Representative SEM image of rMSCs on the PSeD-P scaffold at high magnification at day 14 (magnification 10,000×, scale bar = 2 μm) reveals a unique nanoporous morphology induced by the degradation of PSeD-P, which could facilitate cell-cell interactions and mass exchange.

Interestingly, SEM images of the PSeD-P scaffold with rMSCs seeded after 6 days show that there were nanocrystals on the scaffold (Fig. 7F). EDX analysis revealed that these nanocrystals contained calcium and phosphorus (Fig. 7G). These nanocrystals were totally absent in PSeD scaffolds cultured with rMSCs under identical conditions. This further indicated that the PSeD-P scaffold could promote ECM mineralization.

In addition, a large amount of nanopores with diameters ranging from tens to hundreds of nanometers formed throughout the PSeD-P scaffold within 14 days (Fig. 7C, H). This can likely be ascribed to the degradation of PSeD-P. These nanopores

would be beneficial to the exchange of nutrients and waste and the communication of cells. Furthermore, the structural integrity and macromorphology of scaffolds were maintained well in the presence of nanopores. This ensured continuous mechanical support of the cell culture and made them suitable for later implantation.

4. Discussion

We designed and efficiently synthesized a new phosphorylated polymer, PSeD-P. As expected, PSeD-P showed excellent osteocompatibility. PSeD-P promoted the adhesion, proliferation, and maturation of osteoblasts better than PLGA. PSeD-P also produced significantly higher expression levels of osteogenic biomarker proteins and higher ALP activity in the hMSCs than its non-phosphorylated precursor, PSeD. The results were comparable to having free β-GP in the culture medium. More importantly, without using β-GP, a typical mineralization promoter in osteogenic culture medium, PSeD-P substantially induced mineralization of the ECM of hMSCs, which was completely absent using PSeD under identical culture conditions. In 3D culture, PSeD-P also was a good substrate for the growth and function of rMSCs.

The bioactivity of PSeD-P could be ascribed to the pendent phosphate groups, which have been demonstrated to be key bioactive moieties in phosphorylated polymers.[7,8] Previous studies showed that biomaterials with pendent phosphate groups show faster and more complete mineralization than analogues lacking the phosphorous-containing groups.[31,32] Furthermore, phosphate groups provide an instructive environment for osteogenesis to produce corresponding matrix proteins, such as Col I (Fig. 6A-C) and Runx2 (Fig. 7D-E), which further induce ossification. In addition, negatively charged materials are also known to be good materials to induce bone formation.[33] Polymers that carry negative charges are known to induce more bone formation than neutral polymers.[33-35] More bone formed on negatively charged ceramic surfaces as well.[36] Thus, the negative charges of phosphate groups may also contribute to the enhanced osteoblast and MSCs' maturation and function.

In addition to the pendent phosphate groups, one of the key design features of PSeD-P is the integration of β-GP, a widely used osteogenic molecule. Thus, PSeD-P was expected to have an additional beneficial function based on the β-GP moiety. β-GP plays a key role in providing the essential phosphate group for ECM mineralization as a depot of organic phosphate. Howard Tenenbaum's original observations showed that supplementation of the culture medium with dexamethasone

and β-GP would result in mineralized bone.[37] This has become the popular recipe for osteogenic and mineralization medium. In this medium, dexamethasone initially causes an early increase of osteoblast phenotypic associated proteins[38] and β-GP acts as the provider of the phosphate groups by ALP hydrolysis and also modulates osteoblast activity.[39-42] Phosphate is cleaved from β-GP by the hydrolysis action of ALP, as a cell-mediated process rather than a non-specific process, directly adding phosphate in the culture medium, which may cause improper mineralization. However, frequently adding exogenous β-GP to maintain the phosphate concentration in culture medium is impossible for an *in vivo* study. Due to this limitation, β-GP is now only used for *in vitro* studies. PSeD-P immobilized β-GP in its molecular chain and would gradually release it upon degradation. Thus, PSeD-P could serve as a continuous source of β-GP to promote osteogenesis and mineralization both *in vitro* and *in vivo*.[11] To demonstrate this hypothesis, we compared hMSCs cultured on PSeD-P and PSeD with or without β-GP. Without β-GP, PSeD-P did promote greater expression of an osteogenic biomarker than PSeD without β-GP, comparable to PSeD with β-GP (Fig. 6A-C). The ALP activity of hMSCs on PSeD-P was similar to that of its non-phosphorylated precursor PSeD at an early time point (day 7). However, the ALP activity of hMSCs on PSeD-P considerably increased from day 7 to day 14 and became significantly higher than the activity on PSeD at day 14 (Fig. 6D). This may be partly due to the release of β-GP during the degradation of PSeD-P during long-term culture. In particular, PSeD-P exhibited a substantial ability to promote the extracellular mineralization of hMSCs without the external mineralization promoter β-GP (Fig. 6F). However, there was no detectable extracellular mineralization of hMSCs cultured on PSeD without β-GP (Fig. 6G). These results show that PSeD-P resembled the function of β-GP to some extent and that it had the intrinsic ability to promote osteogenesis and mineralization. This design provides a new strategy to integrate bioactive phosphates via β-GP into biomaterials.

For the past decade, the effects of matrix stiffness and mechano-transduction on cell function and tissue regeneration have been widely appreciated.[43,44] Recently, we demonstrated that the backbone of PSeD-P, PGS, a bioelastomer with a relatively low stiffness, is able to support the osteoblastic phenotype *in vitro*, and we showed that the rabbit ulna can regenerate to repair a critical size defect *in vivo* using this material.[16,17] We concluded that the elasticity and low stiffness of PGS allows a load-transducing milieu, which promotes osteogenesis,

matrix deposition, and eventual bone maturation. A PSeD-P porous scaffold also exhibits excellent elasticity (Fig. 4G). The PSeD-P scaffold also has a modulus of 21.47 ± 1.01 kPa, similar to the PSeD scaffold (21.36 ± 1.97 kPa) and slightly higher than the PGS scaffold (15.00 ± 1.17 kPa), likely due to the more regular structure of PSeD compared to PGS (Fig. 4H).[14] A previous study showed that the fate of mesenchymal stem-cell populations depends on the rigidity of the 3D microenvironment and that osteogenesis occurs predominantly at 11-30 kPa.[45] Accordingly, the moduli of PSe-P, PSeD, and PGS scaffolds are all in this favorable range for osteogenesis. Overall, the PSeD-P scaffold has suitable mechanical properties for bone regeneration.

Phosphorylated polymers are promising biomimetic materials for bone regeneration. However, the existing phosphorylated polymers are usually made of carbon-carbon bonds and are hard to biodegrade. Thus, they are not ideal for use as scaffold materials. Accordingly, we designed a new phosphorylated polymer, PSeD-P, which is completely constructed via hydrolyzable ester bonds from biocompatible small molecules (sebacic acid, glycerol, phosphate). PSeD-P exhibits good biodegradability (Fig. 3) and can be easily processed (Fig. 4A-C). The synthetic method for producing PSeD-P is versatile. The recently developed acid-induced epoxide ring-opening polymerization, which was used to synthesize PSeD, could be readily applied to a wide range of diepoxides and diacids to produce a series of hydroxylated polyesters with diverse structures and properties.[21,46] Furthermore, the phosphorylation method used here is quite simple. Phosphorus oxychloride ($POCl_3$) was the only reagent used aside from the substrate and solvent. The residual $POCl_3$, if any, could be washed out with water right away. The resultant polymers can be easily purified and used for biomedical applications. The concentration of phosphate groups in PSeD-P could be efficiently controlled by varying the feed ratio of $POCl_3$ (these data will be reported later). Overall, we developed a versatile synthetic route to produce biodegradable phosphorylated polymers. Because phosphate groups play important roles in many physiological processes,[7,47] the phosphorylated polymers produced in this way would have great potential in various biomedical applications, not only in bone regeneration.

5. Conclusion

We created a new phosphorylated polymer, PSeD-P, that combines the

osteoconductive backbone PSeD (PGS) and the osteoinductive moiety β-GP. PSeD-P shows excellent compatibility with osteoblasts, and it substantially promotes osteogenesis and the extracellular mineralization of MSCs. To the best of our knowledge, this is the first time that a bioactive polymer for bone regeneration has been produced based on the small molecule β-GP.[48] Using small functional units to control bioactivity represents a powerful method of practically producing therapeutic materials.[12] In addition, PSeD-P shows good degradability and could be readily fabricated on a porous 3D scaffold with a hierarchical porous structure and favorable mechanical properties for osteogenesis. Few existing phosphorylated polymers have similar encouraging properties. Furthermore, the synthetic method is versatile; both the backbone and the concentration of side phosphate groups can be readily tailored to deliver a family of phosphorylated polymers for a wide range of biomedical applications.

Acknowledgments

This research is funded by National High Technology Research and Development Program (863 program, 2015AA020311). National Natural Science Foundation of China (21304015, 81320108010), the Natural Science Foundation of Shanghai (13ZR1401200), China Specialized Research Fund for the Doctoral Program of Higher Education (20130075120009), the Fundamental Research Funds for the Central Universities (2232014A3-01), the State Key Laboratory for Modification of Chemical Fibers and Polymer Materials (Donghua University, LK1412), and the DHU Distinguished Young Professor Program (B201303). We thank Drs. Charles Sfeir and Samer Zaky at the University of Pittsburgh for their productive discussions about MSC culture, Dr Albert D. Donnenberg at the University of Pittsburgh for kindly providing hMSCs.

References

1. J. Henkel, M. A. Woodruff, D. R. Epari, R. Steck, V. Glatt, I. C. Dickinson, P. F. M. Choong, M. A. Schuetz and D. W. Hutmacher, *Bone Res*., 2013, **3**, 216-248.
2. J. Glowacki and E. M. Bueno, *Nat. Rev. Rheumatol*., 2009, **5**, 685-697.
3. C. G. Bellows, J. N. M. Heersche and J. E. Aubin, *Bone and Mineral*, 1992, **17**, 15-29.
4. D. Magne, G. Bluteau, C. Faucheux, G. Palmer, C. Vignes-Colombeix, P. Pilet, T. Rouillon, J. Caverzasio, P. Weiss, G. Daculsi and J. Guicheux, *Journal of Bone and Mineral Research*, 2003, **18**, 1430-1442.
5. A. Gisep, S. Kugler, D. Wahl and B. Rahn, *J Mater. Sci. Mater. Med*., 2004, **15**, 1065-1071.

6. D. Puppi, F. Chiellini, A. M. Piras and E. Chiellini, *Prog. Polym. Sci.*, 2010, **35**, 403-440.
7. B. M. Watson, F. K. Kasper and A. G. Mikos, *Biomedical Materials*, 2014, **9**.
8. J. D. Kretlow and A. G. Mikos, *Tissue Eng.*, 2007, **13**, 927-938.
9. A. C. Allori, A. M. Sailon and S. M. Warren, *Tissue Engineering Part B-Reviews*, 2008, **14**, 259-273.
10. M. M. Stevens and J. H. George, *Science*, 2005, **310**, 1135-1138.
11. D. A. Wang, C. G. Williams, F. Yang, N. Cher, H. Lee and J. H. Elisseeff, *Tissue Eng.*, 2005, **11**, 201-213.
12. D. S. W. Benoit, M. P. Schwartz, A. R. Durney and K. S. Anseth, *Nat. Mater.*, 2008, **7**, 816-823.
13. P. Datta, J. Chatterjee and S. Dhara, *Colloids & Surfaces B Biointerfaces*, 2012, **94**, 177-183.
14. Z. You, H. Cao, J. Gao, P. H. Shin, B. W. Day and Y. Wang, *Biomaterials*, 2010, **31**, 3129-3138.
15. X. Bi, Z. You, J. Gao, X. Fan and Y. Wang, *Acta biomaterialia*, 2014, **10**, 2814-2823.
16. S. H. Zaky, K. W. Lee, J. Gao, A. Jensen, J. Close, Y. D. Wang, A. J. Almarza and C. Sfeir, *Tissue Eng. Pt. A*, 2014, **20**, 45-53.
17. S. H. Zaky, C. K. Hangadora, M. A. Tudares, J. Gao, A. Jensen, Y. D. Wang, C. Sfeir and A. J. Almarza, *Biomedical Mater.*, 2014, **9**, 025003
18. B. P. Chan, T. Y. Hui, M. Y. Wong, K. H. K. Yip and G. C. F. Chan, *Tissue Eng Part C Methods*, 2010, **16**, 225-235.
19. C. D. Hoemann, H. El-Gabalawy and M. D. Mckee, *Pathologie Biologie*, 2009, **57**, 318-323.
20. Z. You and Y. Wang, *Adv. Funct. Mater.*, 2012, **22**, 2812-2820.
21. Z. You, X. Bi and Y. Wang, *Macromol. Biosci.*, 2012, **12**, 822-829.
22. Y. D. Wang, G. A. Ameer, B. J. Sheppard and R. Langer, *Nat. biotechnol.*, 2002, **20**, 602-606.
23. I. Pomerantseva, N. Krebs, A. Hart, C. M. Neville, A. Y. Huang and C. A. Sundback, *J Biomed Mater Res A*, 2009, **91A**, 1038-1047.
24. J. Gao, P. M. Crapo and Y. D. Wang, *Tissue Eng.*, 2006, **12**, 917-925.
25. Z. You, X. Bi, X. Fan and Y. Wang, *Acta Biomater.*, 2012, **8**, 502-510.
26. V. S. Gorantla, S. Schneeberger, L. R. Moore, V. S. Donnenberg, L. Zimmerlin, W. P. Lee and A. D. Donnenberg, *Cytotherapy*, **14**, 104-113.
27. L. Zhang and C. Chan, *Journal of visualized experiments: JoVE*, 2010, DOI: 10.3791/1852.
28. R. S. Tuan, *Molecular Therapy*, 2003, **7**, S106-S106.
29. B. J. Slater, M. D. Kwan, D. M. Gupta, N. J. Panetta and M. Longaker, *Expert Opinion on Biological Therapy*, 2008, **8**, 885-893.
30. T. E. England, J. Samsoondar and G. Maw, *Clin. Biochem.*, 1994, **27**, 187-189.
31. I. C. Stancu, R. Filmon, C. Cincu, B. Marculescua, C. Zaharia, Y. Tourmen, M. F. Basle and D. Chappard, *Biomaterials*, 2004, **25**, 205-213.
32. Y. J. Yin, X. Y. Luo, J. F. Cui, C. Y. Wang, X. M. Guo and K. D. Yao, *Macromolecular Bioscience*, 2004, **4**, 971-977.
33. F. R. Baxter, C. R. Bowen, I. G. Turner and A. C. E. Dent, *Annals of Biomedical Engineering*, 2010, **38**, 2079-2092.
34. A. Chierico, R. Valentini, Z. Majzoub, A. Piattelli, A. Scarano, L. Okun and G. Cordioli, *Clin Oral Implants Res*, 1999, **10**, 415-424.
35. B. Callegeri and W. D. Belangero, *Acta Orthop Bras*, 2004, **12**, 160-166.
36. S. Nakamura, T. Kobayashi and K. Yamashita, *J. Biomed. Mater. Res.*, 2002, **61**, 593-599.
37. H. C. Tenenbaum, *J Dent Res*, 1981, **60**, 1586-1589.
38. B. D. Boyan, Z. Schwartz and A. L. Boskey, *Bone*, 2000, **27**, 341-342.
39. F. Anagnostou, C. Plas, J. R. Nefussi and N. Forest, *Journal of Cellular Biochemistry*, 1996, **62**, 262-274.
40. G. R. Beck, E. Moran and N. Knecht, *Experimental Cell Research*, 2003, **288**, 288-300.
41. N. Fratzl-Zelman, P. Fratzl, H. Horandner, B. Grabner, F. Varga, A. Ellinger and K. Klaushofer, *Bone*, 1998, **23**, 511-520.
42. J. R. Porter, T. T. Ruckh and K. C. Popat, *Biotechnology Progress*, 2009, **25**, 1539-1560.

43. A. J. Engler, S. Sen, H. L. Sweeney and D. E. Discher, *Cell*, 2006, **126**, 677-689.
44. D. E. Discher, P. Janmey and Y. L. Wang, *Science*, 2005, **310**, 1139-1143.
45. N. Huebsch, P. R. Arany, A. S. Mao, D. Shvartsman, O. A. Ali, S. A. Bencherif, J. Rivera-Feliciano and D. J. Mooney, *Nat*. *Mater.*, 2010, **9**, 518-526.
46. Z. You and Y. Wang, in *Biomaterials for tissue engineering applications: a review of the past and future trends*, eds. J. Burdick and R. L. Mauck, Springer-Verlag/Wien, 2011, ch. 4, pp. 75-118.
47. Y. G. Ko and P. X. Ma, *J. Colloid Interface Sci.*, 2009, **330**, 77-83.
48. F. R. Maia, S. J. Bidarra, P. L. Granja and C. C. Barrias, *Acta Biomater.*, 2013, **9**, 8773-8789.

One sentence for highlighting the novelty of the work:
This study demonstrates a simply powerful way to make therapeutic materials: using small functional units (phosphates) to control bioactivity (osteogenesis).